Electronic Supplementary Information

Hexaazatriphenylene-based polymer cathode for fast and stable lithium-, sodium- and potassium-ion batteries

Roman R. Kapaev[1, 2, 3] **, Ivan S. Zhidkov*[4]*, Ernst Z. Kurmaev*[4,5]*, Keith J. Stevenson*[1]*, Pavel A. Troshin*[1, 2]

[1] Center for Energy Science and Technology, Skolkovo Institute of Science and Technology, Nobel str. 3, Moscow 143026, Russia

[2] Institute for Problems of Chemical Physics RAS, Acad. Semenov str. 1, Chernogolovka 142432, Russia

[3] D.I. Mendeleev University of Chemical Technology of Russia, Miusskaya sq. 9, Moscow 125047, Russia

[4] Institute of Physics and Technology, Ural Federal University, Mira str. 19, Yekaterinburg 620002, Russia

[5] M.N. Mikheev Institute of Metal Physics of Ural Branch of Russian Academy of Sciences, S. Kovalevskoi str. 18, Yekaterinburg 620108, Russia

*E-mail: roman.kapaev@skoltech.ru

Table S1. Elemental composition of **P1**.

Entry	H (wt. %)	C (wt. %)	N (wt. %)	C:H (at. ratio)	C:N (at. ratio)
Experimental	3.97	64.25	17.81	1.34	4.2
Theoretical $C_{24}N_6H_9$	2.38	75.59	22.03	2.7	4.0
Theoretical $C_{24}N_6H_9(H_2O)_4$	3.78	63.57	18.53	1.4	4.0

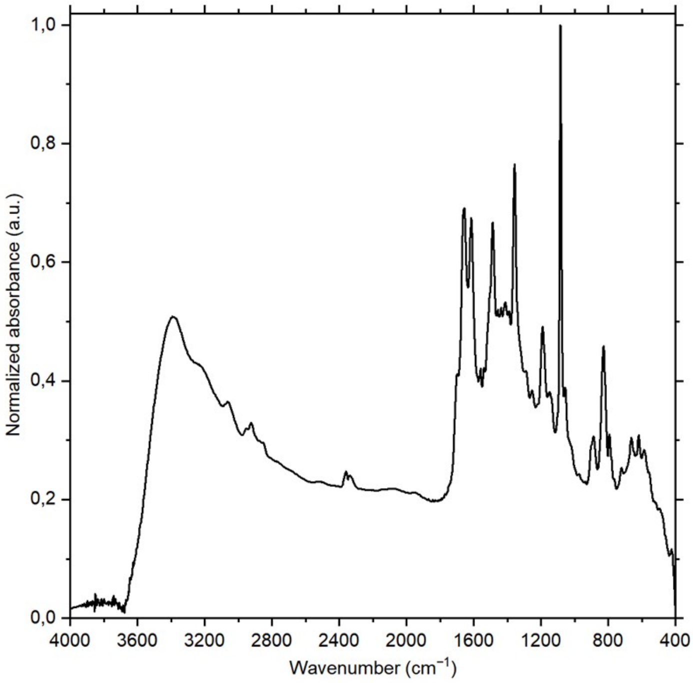

Figure S1. FTIR spectrum of **P1**.

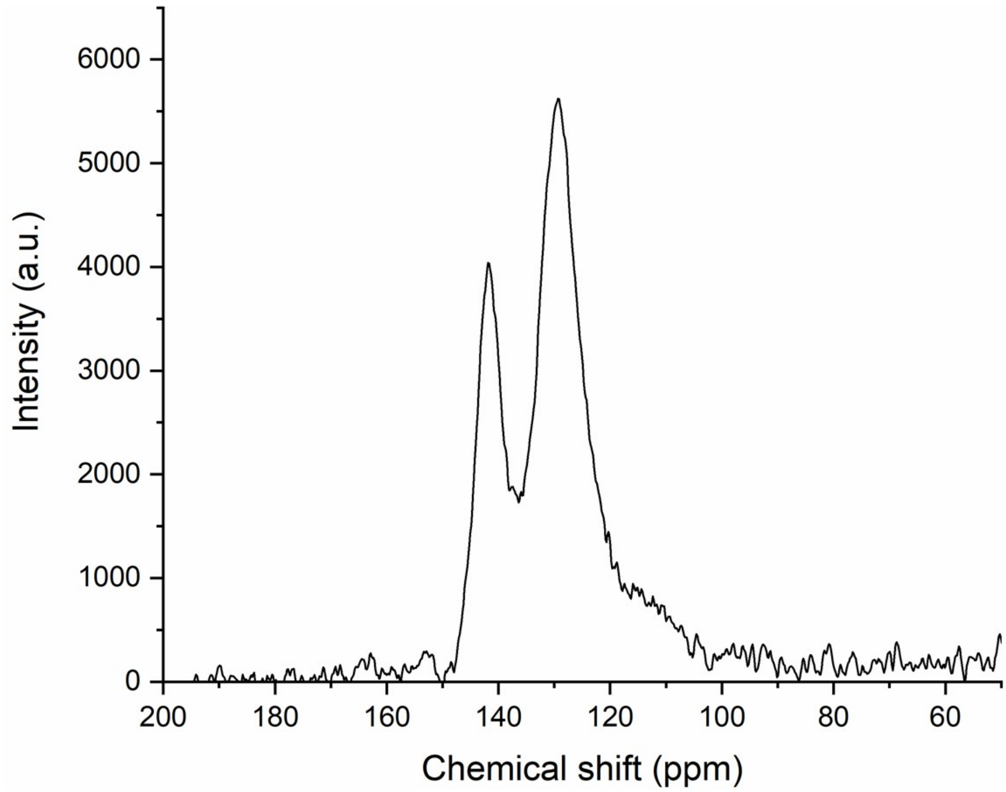

Figure S2. Magic-angle spinning solid-state ^{13}C NMR spectrum of **P1**.

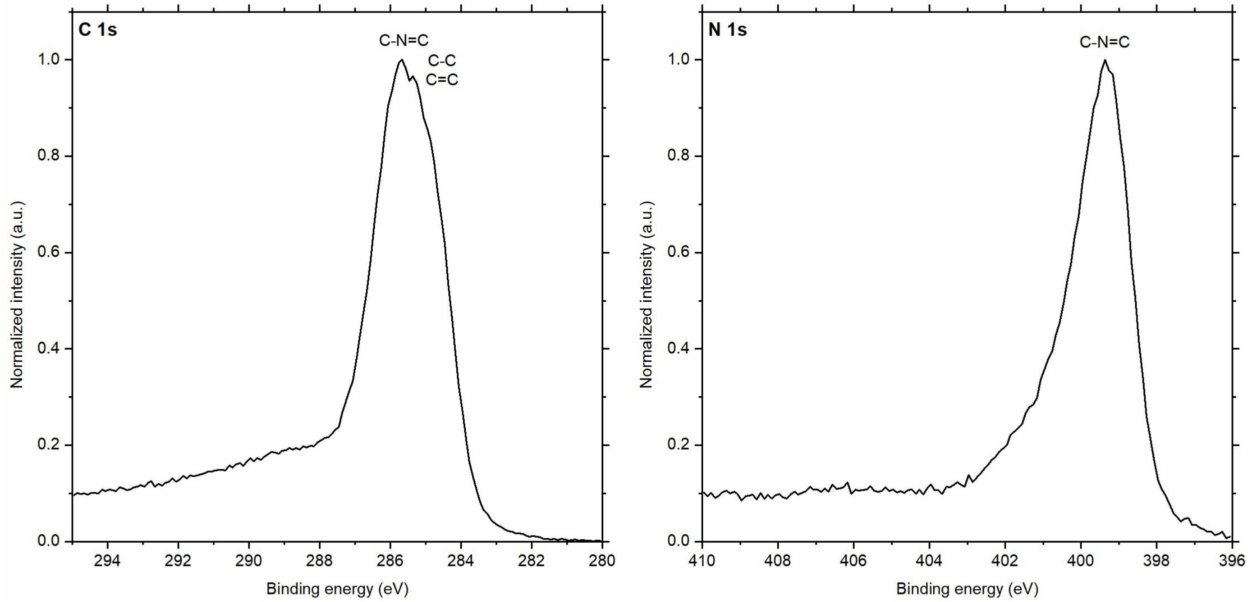

Figure S3. C 1s and N 1s X-ray photoelectron spectra of **P1**.

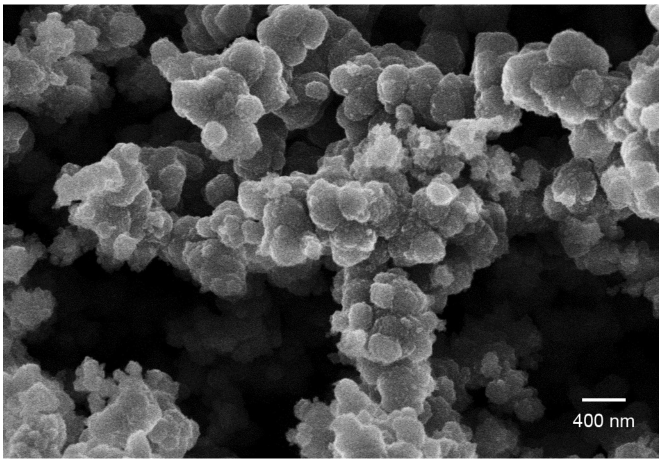

Figure S4. SEM image of **P1**.

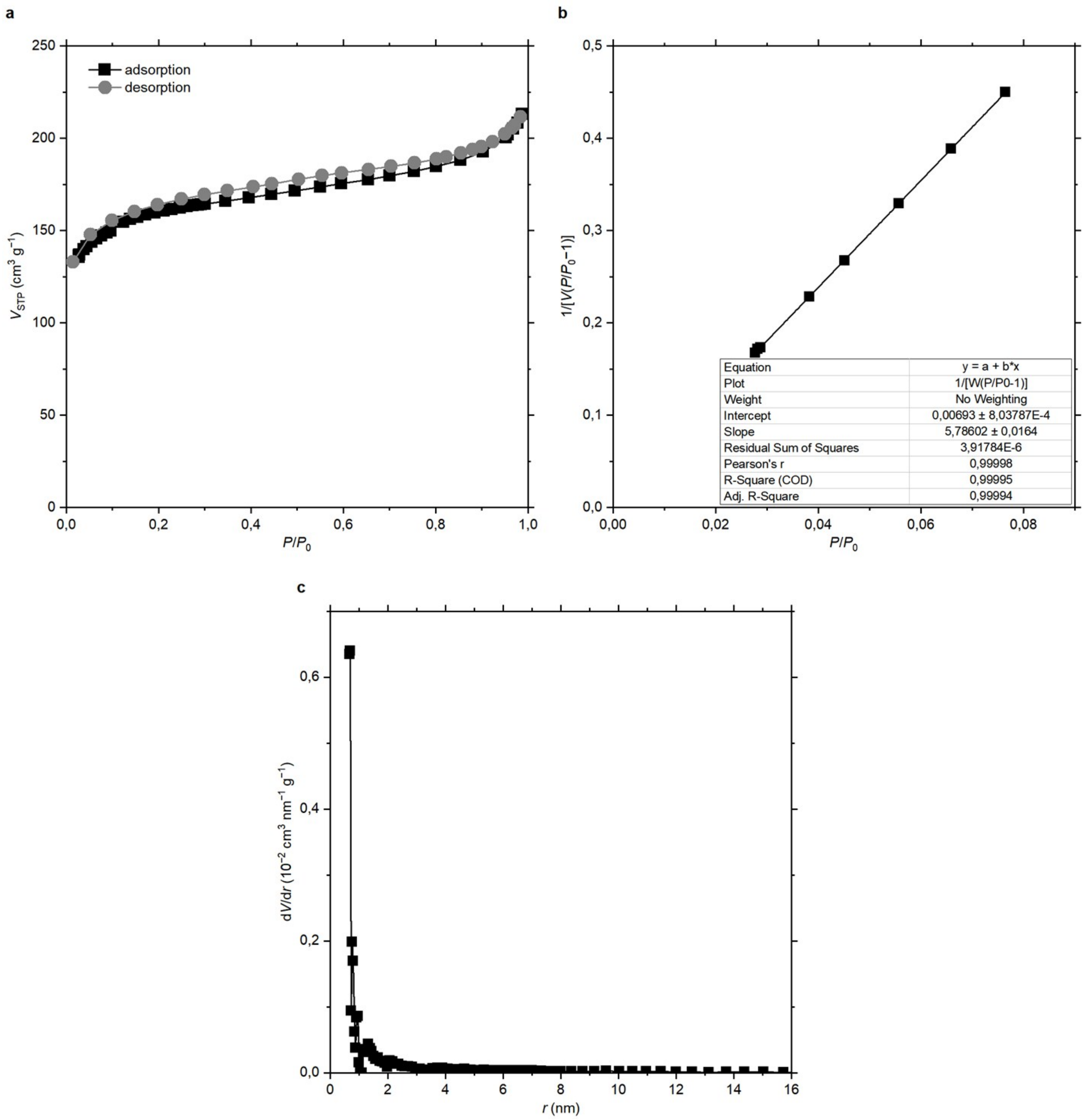

Figure S5. (a) Adsorption-desorption isotherms of **P1**, (b) plot for BET surface area calculation, (c) pore size distribution calculated by NLDFT method from the desorption curve.

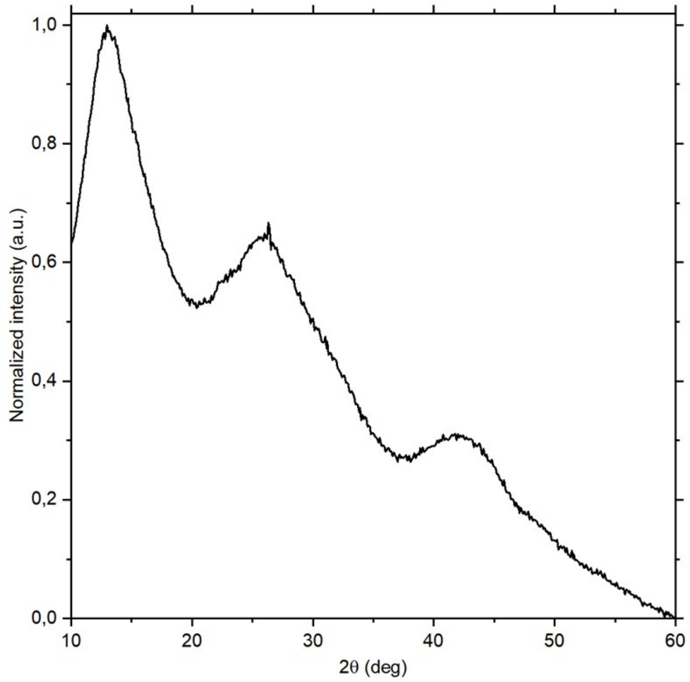

Figure S6. Powder XRD pattern of **P1**.

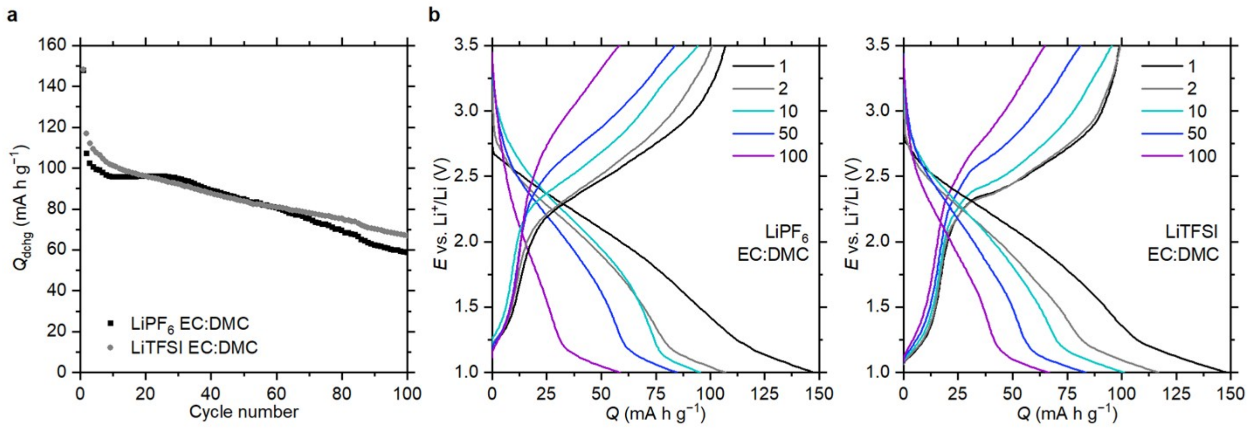

Figure S7. Cycle performance of **P1** in LIBs with 1 M $LiPF_6$ or 1 M LiTFSI in EC:DMC: (a) cycling stability at 500 mA g^{-1}; (b) charge-discharge curves at 500 mA g^{-1} for different cycle numbers.

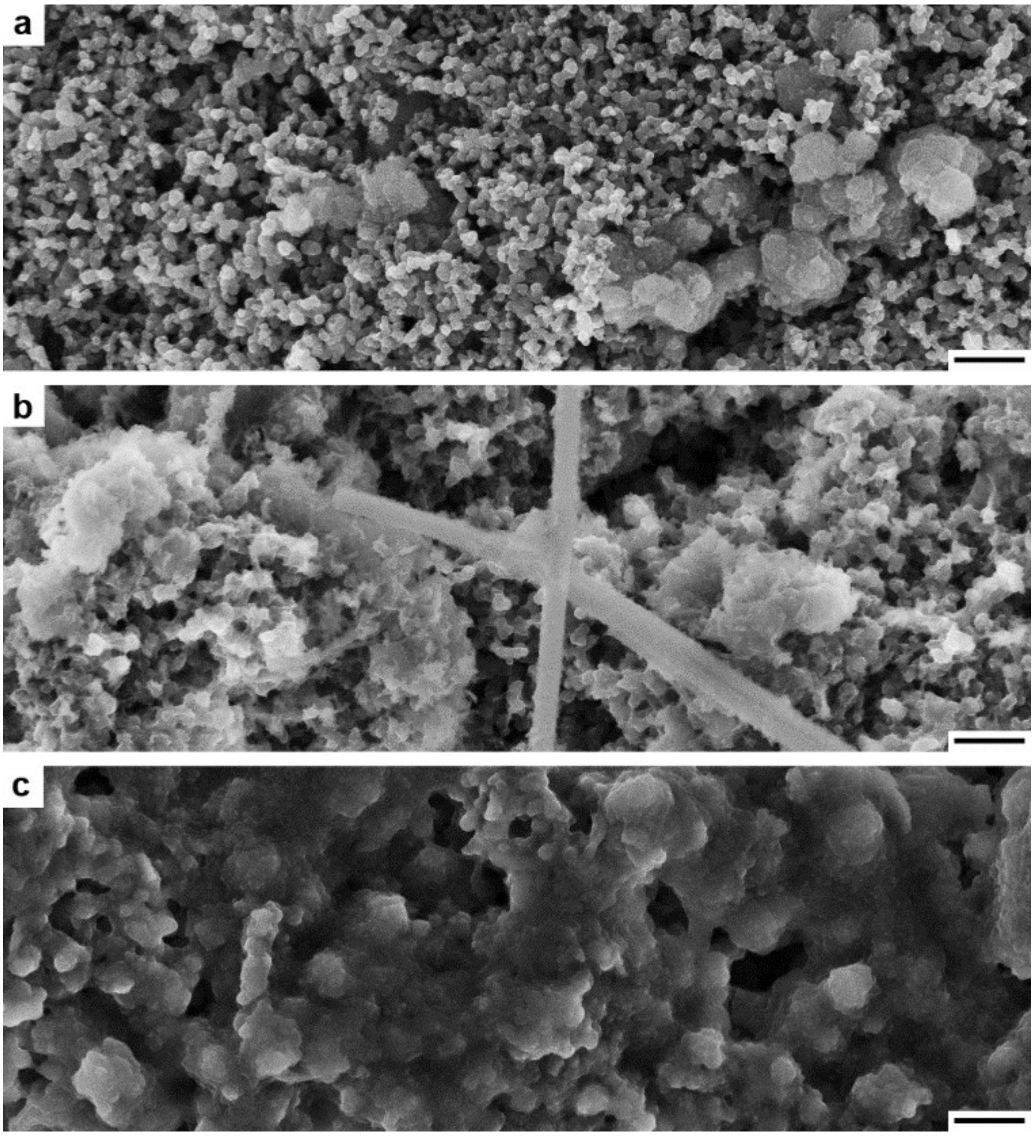

Figure S8. SEM images of the electrodes (a) before cell assembling and after 100 cycles at 500 mA g^{-1} in (b) 1ᴍ LiTFSI DME, (c) 1ᴍ LiTFSI EC:DMC. Scale bars: 400 nm. Two filaments observed in (b) are fibers from the separator.

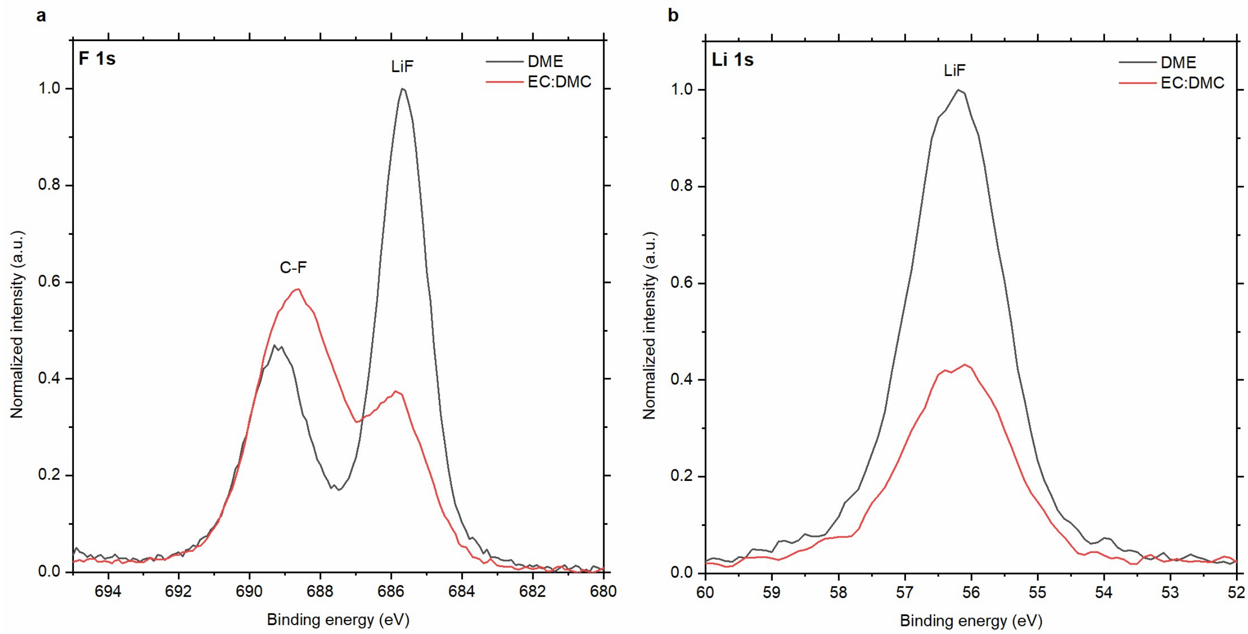

Figure S9. (a) F 1s and (b) Li 1s XPS spectra of the electrodes after 100 cycles at 500 mA g^{-1} in 1ᴍ LiTFSI DME or 1ᴍ LiTFSI EC:DMC.

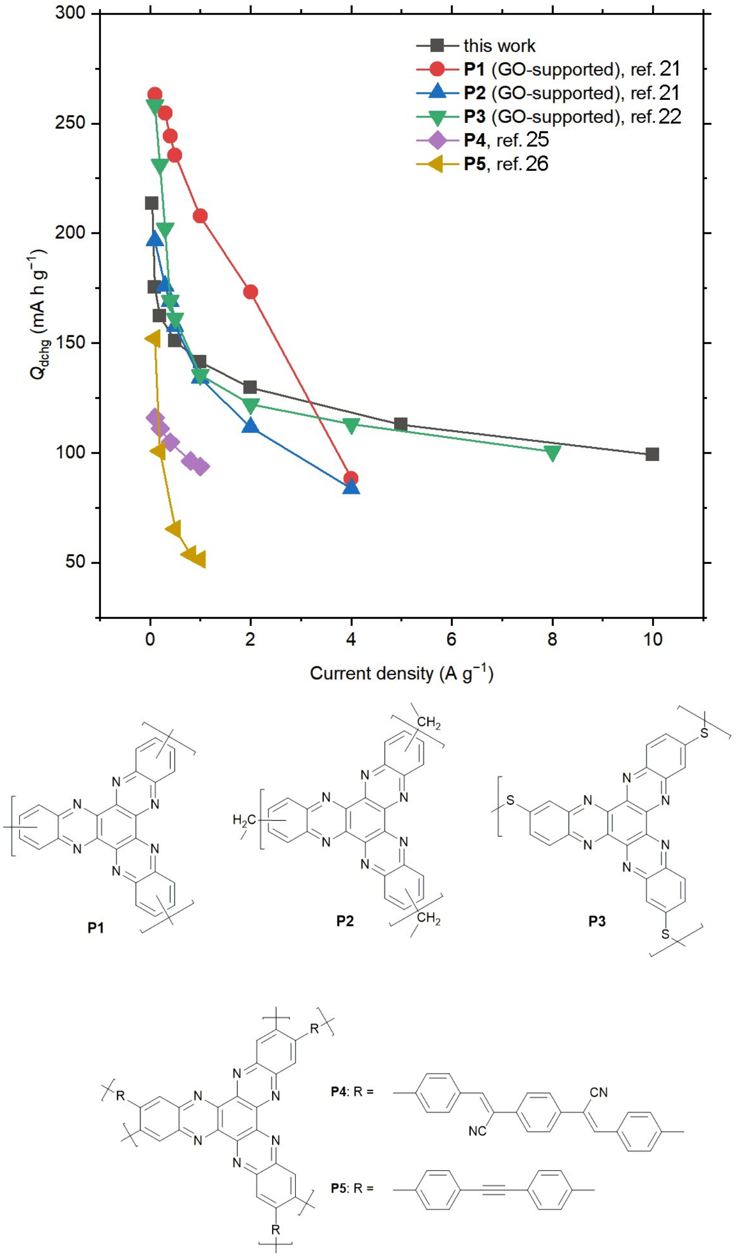

Figure S10. Rate performance of **P1** reported in this paper compared to the published data for HAT-based polymers in LIBs.

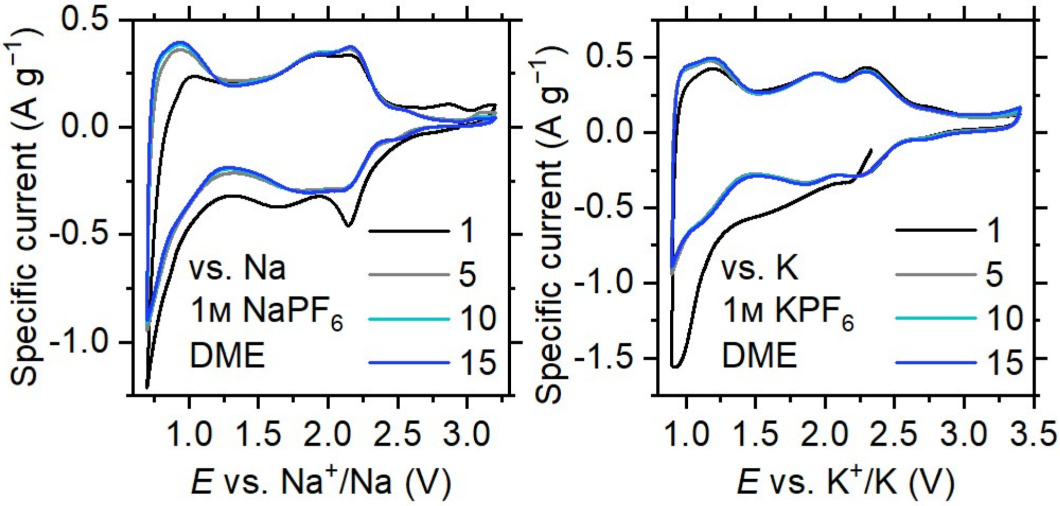

Figure S11. CVs of **P1** in sodium- and potassium-ion cells measured at 1 mV s^{-1} scan rate for different scan numbers.

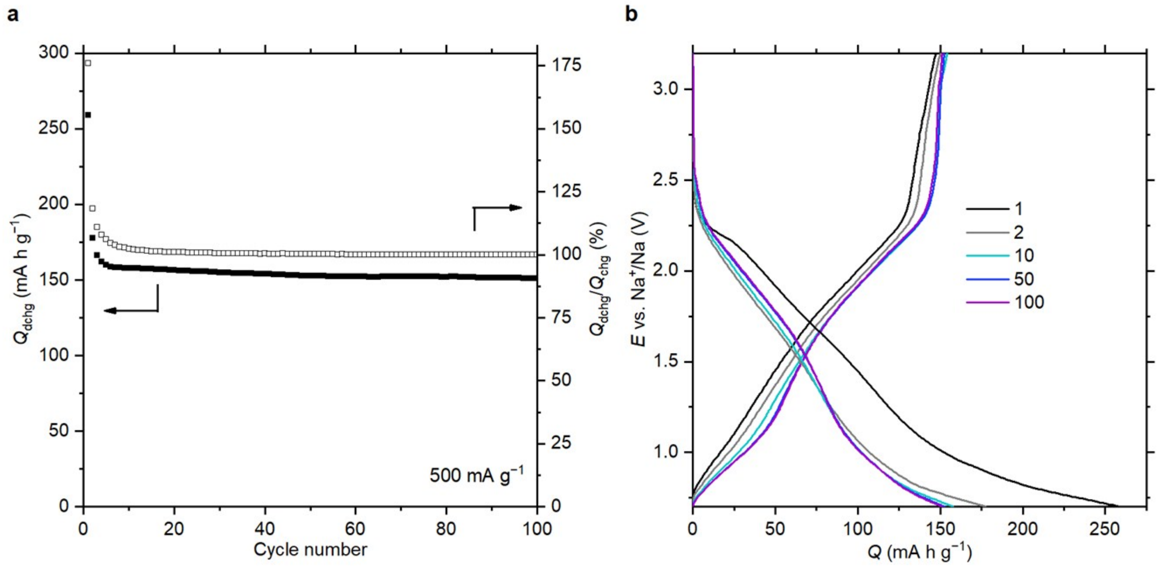

Figure S12. Cycling performance of **P1** in SIBs at 500 mA g^{-1}: (a) the dependence of the discharge capacity and the coulombic efficiency on the cycle number; (b) charge-discharge curves for different cycle numbers.

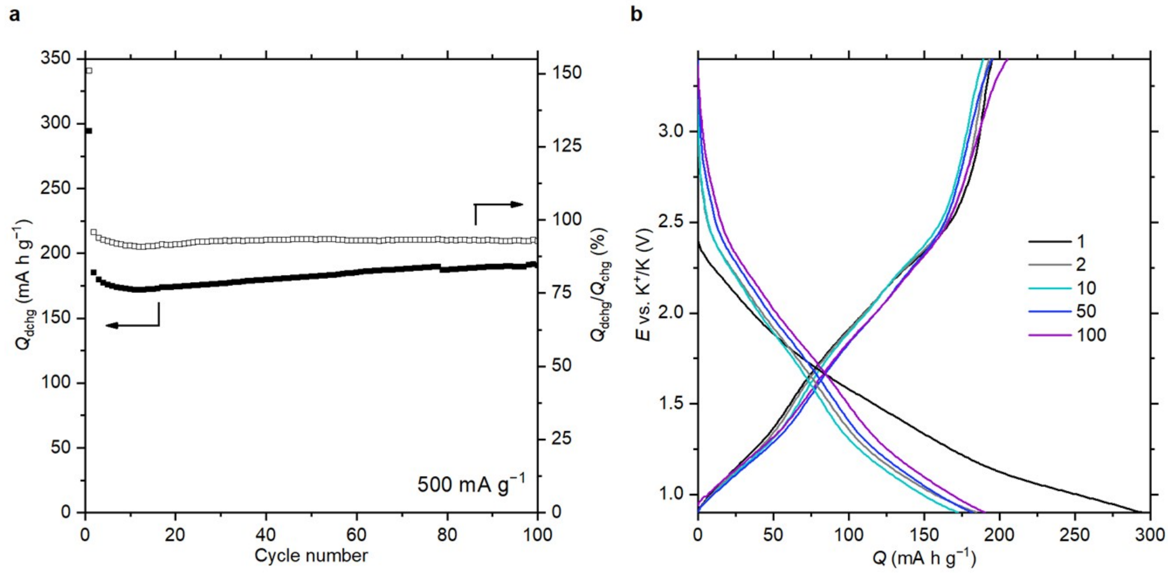

Figure S13. Cycling performance of **P1** in PIBs at 500 mA g^{-1}: (a) the dependence of the discharge capacity and the coulombic efficiency on the cycle number; (b) charge-discharge curves for different cycle numbers.

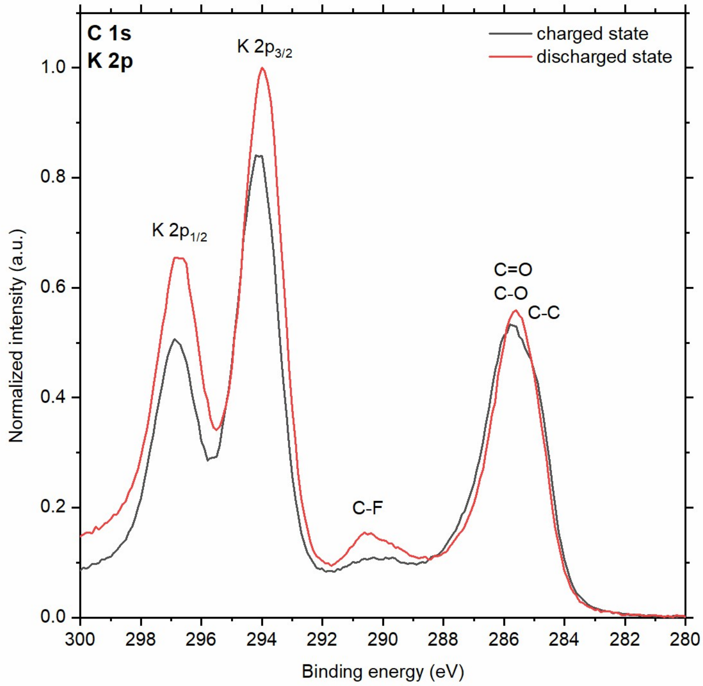

Figure S14. XPS C 1s and K 2p for the electrodes in the charged (to 3.4 V vs. K^+/K) and discharged (to 0.9 V vs. K^+/K) states after one charge-discharge cycle at 50 mA g^{-1}. The electrodes were washed with dry 1,2-dimethoxyethane prior to measurements.

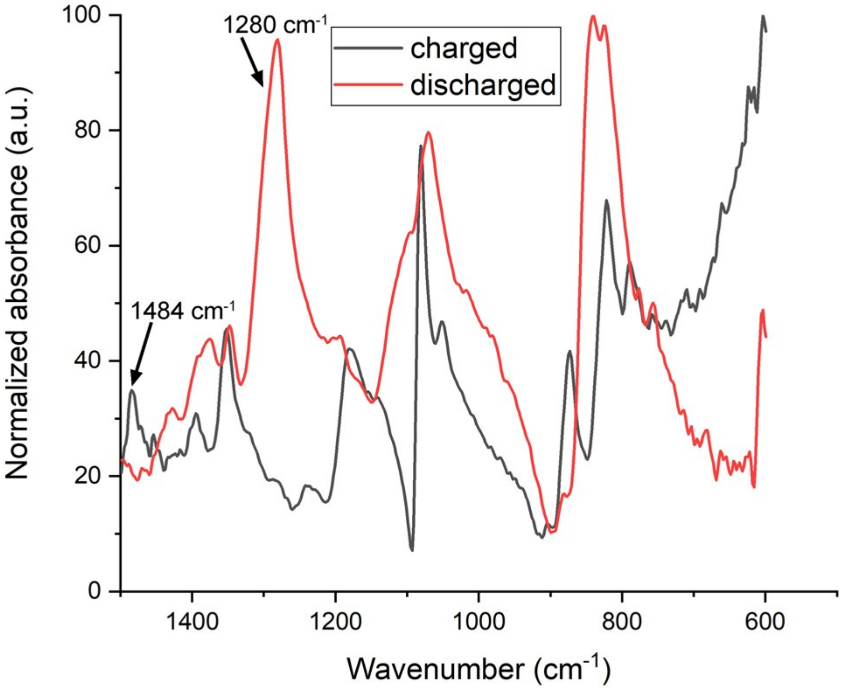

Figure S15. FT-IR spectra of **P1**-based electrodes in charged and discharged states (K-ion batteries). The electrodes of the disassembled cells were washed with dimethoxyethane and dried in Ar-filled glovebox prior to measurements.

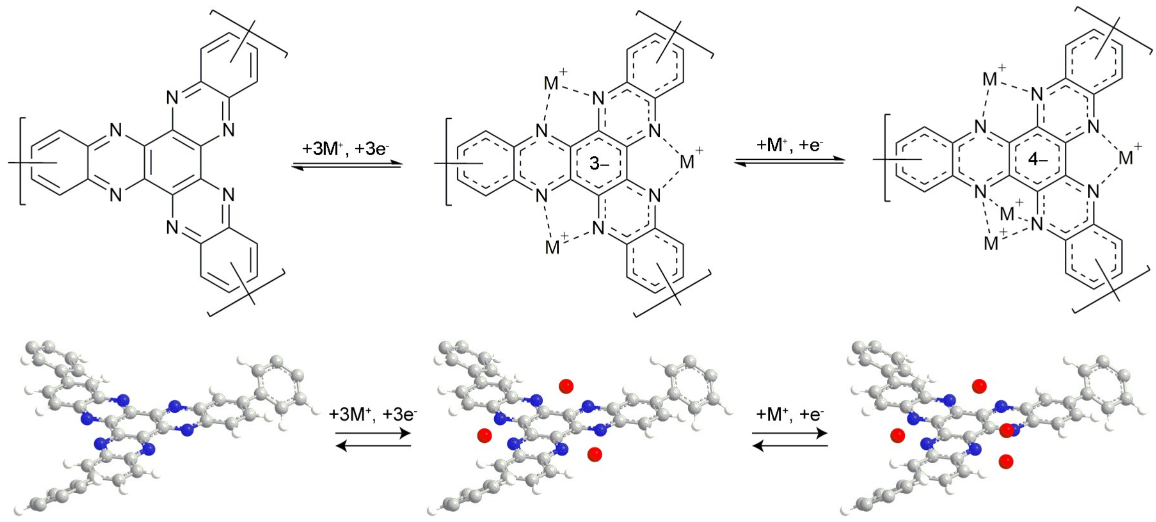

Figure S16. Proposed charge-discharge mechanism for **P1** structure unit.

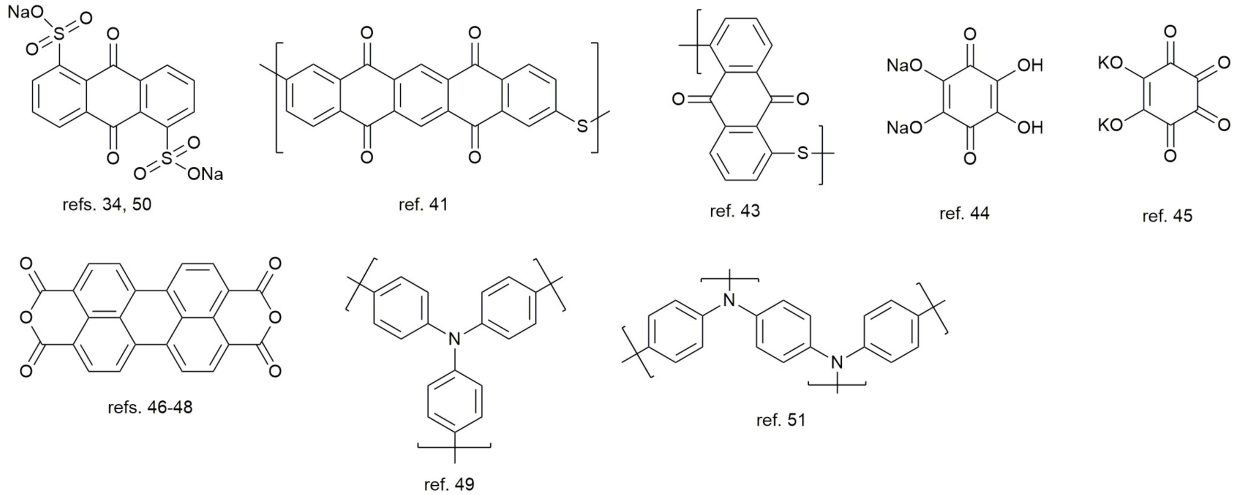

Figure S17. Molecular structures of organic cathodes for potassium-ion batteries reported in the literature.

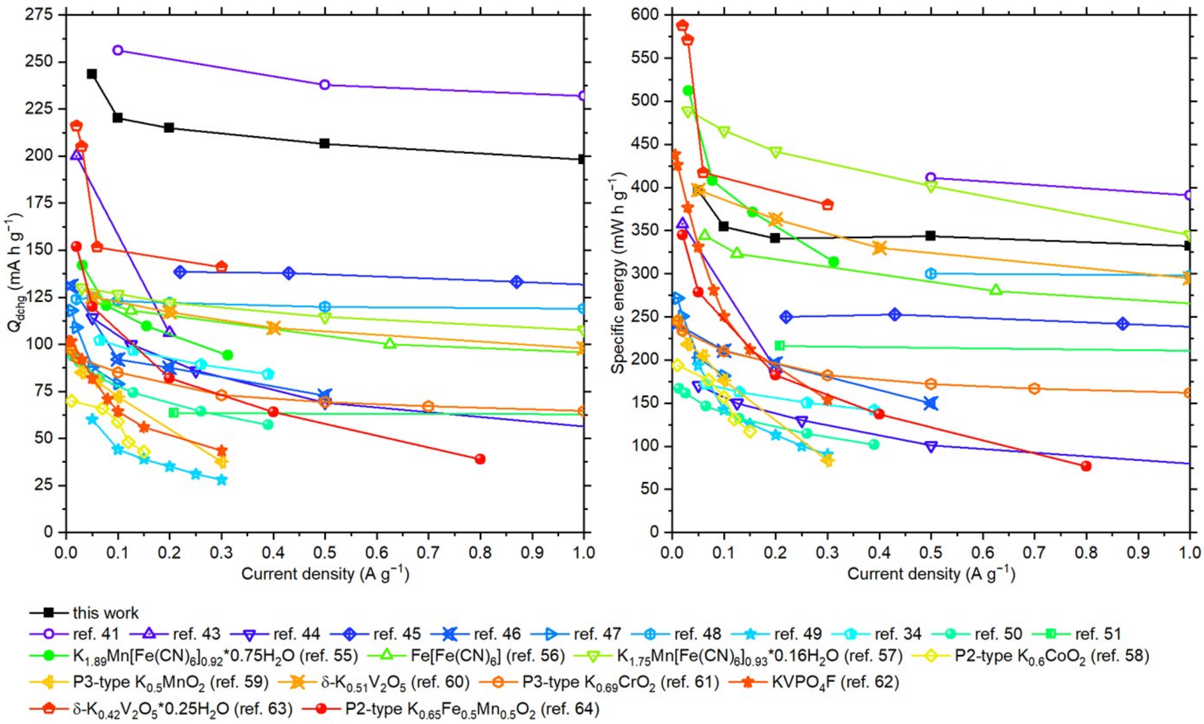

Figure S18. Rate performance of **P1** cathode achieved in this work in comparison with the reported cathodes for PIBs. These plots are expanded 0–1 A g^{-1} regions of Figure 5d.

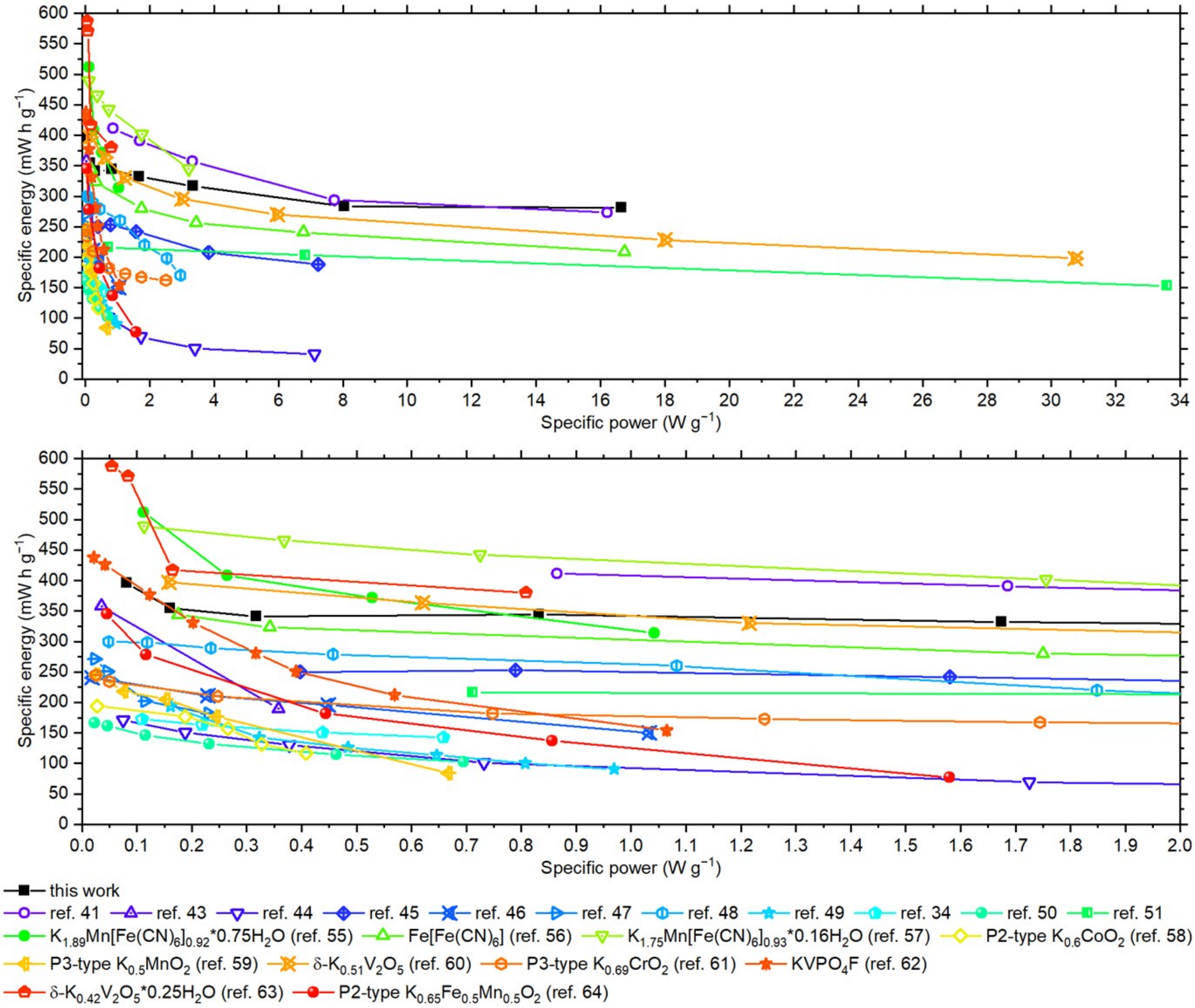

Figure S19. The dependence of the energy density on the power density for **P1** and the reported cathodes for PIBs. The lower plot is an expanded 0–2 W g^{-1} region of the upper plot.

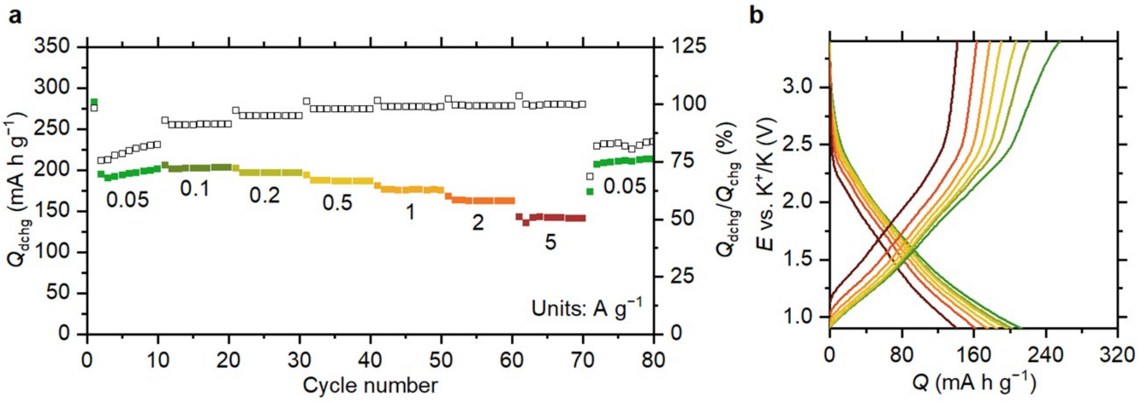

Figure S20. Electrochemical behavior of P1 in potassium-ion batteries for an electrode with the mass ratio of P1:Super P:PVdF = 6:3:1. (a) discharge capacities and charge/discharge capacity ratios at different current rates; (b) charge-discharge curves for each 10th cycle represented in (a) except for the cycle 10.

Table S2. Cycling performance of **P1** in K-ion batteries in comparison with the PIB organic cathodes published in the literature. The data on the inorganic cathode materials are available in the reviews.[42, 43]

Reference number	Current density (A g^{-1})	Number of cycles	Capacity decay (%)
This work	10	4600	No decay
This work	0.5	100	No decay
41	5	3000	~5 [a]
43	0.02	50	25
44	0.2	200	23
44	0.025	100	~70
45	0.435	100	33
46	0.05	200	~23
47	0.02	40	~48
48	0.1	140	No decay
48	1	1000	13.3
49	0.1	500	24.5
34	0.39	1000	20
50	0.013	100	No decay [b]
51	0.209	500	15
51	2.09	1000	37
51	10.45	1000	80

[a] 100% of the capacity was set to 200 mA h g^{-1} (according to the authors, by reaching this value the fast degradation stopped)

[b] The capacity observed at the second cycle was set to 100%